



Application of Endurance Time Method for the Seismic Assessment of an Isolated Viaduct

Hamidreza Nemati¹, Arash Poursadrollah², Javad Katebi¹, Mario D’Aniello², Raffaele Landolfo², Arash Bahar³

¹Department of Civil Engineering, University of Tabriz, Tabriz, Iran

²Department of Structures for Engineering and Architecture, University of Federico II, Naples, Italy

³Department of Civil Engineering, University of Guilan, Guilan Province, Rasht, Iran

SUMMARY: *Endurance Time (ET) method is a dynamic analysis in which the structures are subjected to a predefined intensifying acceleration. The inherently dynamic nature of ET makes it applicable for various types of structures with different heights and degrees of freedom. The purpose of this study is to investigate the feasibility of ET method for analyzing an isolated bridge under different controlled systems. The optimal control force is calculated using both the Linear Quadratic Regulator (LQR) algorithm and Continuous Sliding Mode Control (CSMC). To this end, a five-span isolated viaduct is selected as a case study. Column-isolator-deck system is idealized as a two-degree-of-freedom lumped mass model. Three distinct control strategies are used including active, semi-active, and passive control systems. The deck displacements obtained from ET method are compared against the results of conventional time history analysis for different excitation levels. The ET results show good accuracy in predicting the seismic behavior of isolated bridge under different controlled systems. On top of that, this method substantially reduces the computational demands contrary to time history analysis.*

KEYWORDS: *endurance time method, nonlinear isolated bridge, active and semi-active control, time history analysis*

1 Introduction

Existing bridges and viaducts are crucial infrastructures that can be highly vulnerable to seismic events. To mitigate the induced seismic actions on these structures, one of the most popular approaches is to use seismic isolation technology as a passive device. The performance of the isolated bridges against severe ground motions has been recently investigated by several researchers [Shen et al. 2004, Liao et al. 2004, Bedon and Morassi 2014, Losanno et al. 2017]. It was observed that piers and isolators undergo high deformation demand, which may lead to excessively large deck displacements [Lee and Chen 2011, Lee and Kawashima 2006, Mao et al. 2017]. Consequently, several attempts have been made to combine smart materials with these isolators as a retrofit technique in different structures

[Fraternali et al. 2018, Corbi et al. 2019, Terenzi et al. 2019, Gabbianelli et al. 2020, Bernuzzi et al., 2021].

However, beyond the selection of the most appropriate design/retrofit strategy, choosing the appropriate analyzing method is a major concern when it comes to evaluating the seismic response of these structures. Seismic design of structures requires a quantitative understanding of response at different performance levels, ranging from nearly elastic behavior to highly inelastic behavior associated with incipient collapse. While different approaches (e.g., equivalent lateral forces, response spectrum, multi-mode pushover analysis, and time history analysis) have been largely adopted in the past [See Montuori et al. 2021, Ferraioli et al. 2018, Colajanni et al. 2017], even accounting for the inelastic behavior of structures, the development of a robust method to predict the inelastic seismic behavior of structures remains a challenge. In seismically active regions, the design of critical structures such as power plants, dams, tall buildings, and cable-stayed bridges is usually based on a complete time history analysis. Although this analysis is the most reliable method, it is the most time-consuming one compared to other methods. Furthermore, it can be challenging to select a suite of ground motions where the median response spectrum is consistent with a specified target spectrum [Zanini et al. 2017]; especially when the pool of available records is limited by source-site characteristics due to the disaggregation of seismic hazard and insufficient number of accelerograms in the design location [Basim et al. 2018]. Nowadays, the Endurance Time (ET) method is known as a new and innovative approach as a suitable alternative to the different available procedures [Estekanchi et al. 2007]. In this method, an intensifying dynamic excitation is used as a loading function. To this end, the structural responses at different excitation levels are obtained in a single time history analysis [Estekanchi et al. 2007]. The potential benefits of this approach are demonstrated and explored in detail in the next sections of this paper.

The application of this method in linear and nonlinear seismic analysis of structures has been studied before. For example, Mirzaee and Estekanchi (2015) investigated the seismic response of different steel moment frames by the ET method, and different response parameters obtained by ET method were compared with those calculated by time history analysis. Furthermore, this method has been applied to different structures with different complexity. For instance, Estekanchi and Alembagheri (2012) examined the seismic assessment of anchored and unanchored steel tanks using the ET method, which results in an acceptable estimation of different demand parameters. However, these studies do not address the application of ET method to different control systems. Therefore, this study focuses on the application of the ET method for the seismic assessment of different control systems applied on an isolated viaduct. Active, passive, and semi-active control are alternatively used to mitigate the seismic effects on the structure. Active control systems use the external power to generate the control force, and the control force is determined by a control algorithm with a measured structure response. This control system theoretically has the highest versatility and adaptability among the others. However, a large power supply is required, which may not be supplied due to electricity breakdown [Franklin et al. 2008]. Passive control systems, on the other hand, use passive energy-dissipation devices and are less adaptive instead. Semi-active control systems have the features of both active and passive control i.e., it provides the reliability of passive devices and adaptability of active control systems without requiring an ample power supply [Franklin et al. 2008].

2 Endurance Time method

ET method is a type of dynamic analysis in which the structure is subjected to intensifying acceleration functions, and its performance is monitored at different excitation levels. A schematic representation of ET analysis for three prototype structures is shown in Figure 1.

These structures are excited to an ET acceleration function, and their performances are recorded during the analysis. Since these accelerations are produced in such a way that the amplitude of the acceleration is increased with time, structures gradually go from elastic to nonlinear inelastic phase. Depending on the dynamic features of the structures, their responses differ at different hazard levels. Different structural responses including displacements, drift ratios, stresses, plastic rotations, or other appropriate Engineering Demand Parameters (EDPs) can be selected as intensity measure and monitored through the analysis.

ET acceleration functions are generated in a way that at a specific time, t_{target} , the response spectrum matches a pre-specified reference response spectrum, and it proportionally intensifies to the time for the rest of the time range. Hence, the target acceleration response of ET accelerogram is defined in Equation (1):

$$S_{aT}(T, t) = S_{ac}(T) \times \frac{t}{t_{target}} \quad (1)$$

where $S_{aT}(T, t)$ is the target acceleration response at time t , T is the period of free vibration, and S_{ac} is the target acceleration spectrum [Estekanchi et al. 2007].

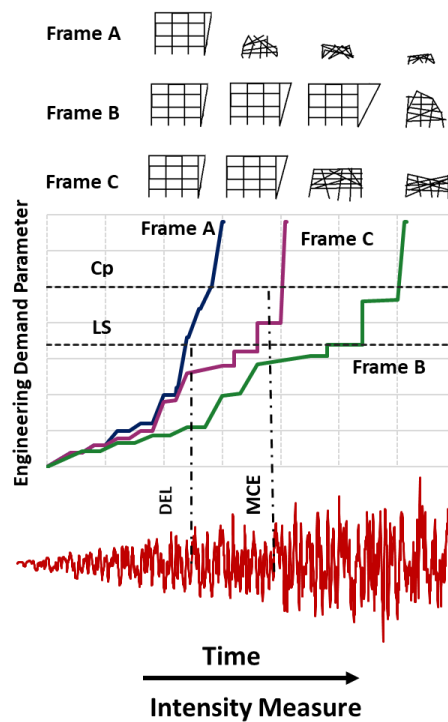


Figure 1 - Schematic representation of ET analysis and its application in PBEE [Riahi and Estekanchi 2011]

In Equation (1), the response spectrum at each time is proportional to the target spectrum multiplied by a scaling factor. The scaling factor linearly increases with time and is equal to unity at t_{Target} . To improve the accuracy of the analysis, the average of the results from at least three accelerograms should be used. The results of ET method are usually interpreted using ET response curve. The value of intended EDP at each time, t , is the maximum absolute of the results from 0 to t .

One of the main goals of this study is to investigate the feasibility of ET method by comparing analysis results against the response of structures subjected to ground motions. The average of seven ground motions recorded on a stiff soil conditioned [Estekanchi et al. 2011] was used as the target response spectrum. These ground motions were selected among the 20 records used in FEMA440 (2005). Seven records with the most compatible response spectra shapes to the response spectrum of type II of Iranian Seismic Standard (ISS 2800) (2015) were selected. It should be noted the ET concept is not feasible to be used in near field where structures are most likely to experience forward directivity effect. Figure 2a presents the smooth average of the acceleration spectrum of these scaled records.

Table 1 shows the properties of these earthquakes. Figure 2b illustrates the response spectra of this set of three ET acceleration functions at $t = 5, 10, 15$ seconds, along with the average of the seven ground motions multiplied to their equivalent scale factor.

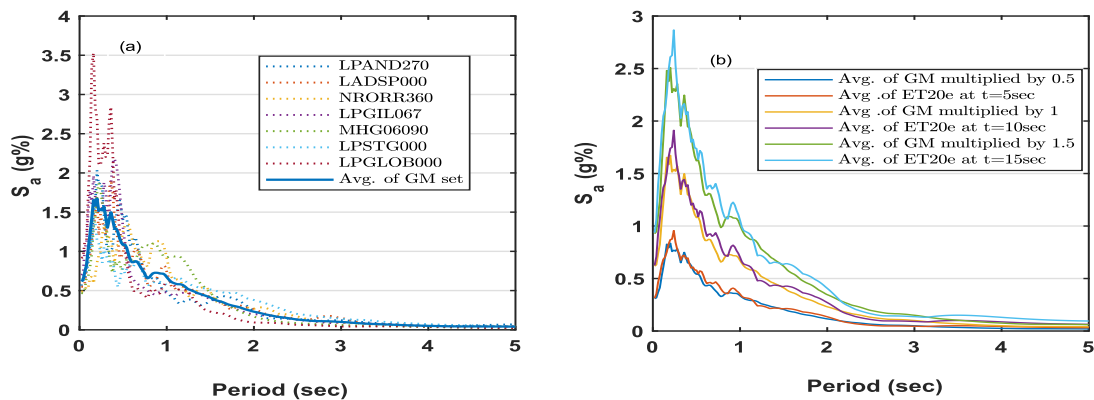


Figure 2 - Acceleration response spectra: (a) Seven scaled ground motions of GM set and their average; (b) Average at different time and corresponding response spectra of GM set

Table 1 - properties of selected ground motions

Date	Earthquake Name	Magnitude (Ms)	Station Number	Component (deg)	PGA (cm ² /sec)	Abbreviation
06/28/92	Landers	7.5	12 149	0	167.8	LADSP000
10/17/89	Loma	7.1	58 065	0	494.5	LPSTG000
10/17/89	Loma	7.1	47 006	67	349.1	LPGIL067
10/17/89	Loma	7.1	58 135	360	433.1	LPGLOB000
10/17/89	Loma	7.1	1 652	270	239.4	LPAND270
04/24/84	Morgan	6.1	57 383	90	280.4	MHG06090
01/17/94	Northridge	6.8	24 278	360	504.2	NRORR360

An example of the ET Acceleration Function (ETAF) from this family is shown in Figure 3a. These figures illustrate the linear intensifying trend with the time passage. The ET Velocity Function (ETVF) for the considered ETAF is shown in Figure 3b.

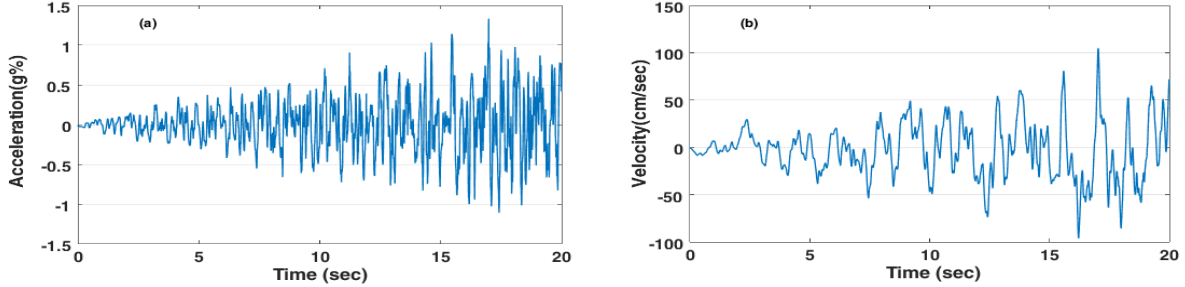


Figure 3 - Acceleration and velocity of ET (a) Simple ETFA from e-series; (b) Corresponding ETVF from e-series

3 Control Systems

3.1 Motion Equation of Control Systems

The Equation of motion for a nonlinear structure with n-degrees of freedom using a certain control system is given as follows:

$$[M]\{\ddot{x}(t)\} + [C]\{\dot{x}(t)\} + F_s[x(t)] = [\gamma]\{u(t)\} + \{\delta\}\ddot{x}_g(t) \quad (2)$$

in which $x(t)$ is an n-vector indicating drift of the stories, M and C are $(n \times n)$ mass and damping matrices, respectively. The control vector $u(t) = [u_1, u_2, \dots, u_r]^T$ consists of r arrays; γ is an $(n \times r)$ matrix which denotes the location of r controllers; $\{\delta\}$ is an n-vector denoting the influence of the ground motion excitation and F_s is an n-vector denoting the nonlinear stiffness force which is assumed to be a function of $x(t)$. As yielding occurs, the hysteretic stiffness of each degree of freedom can be modeled in accordance with Faycal and Joze (2007), as follows:

$$FS_i = \alpha_i k_i x_i(t) + (1 - \alpha_i) k_i D_{yi} v_i \quad (3)$$

where v_i is an n-dimensional evolutionary hysteretic vector whose i^{th} component is given by the Bouc–Wen model as [Faycal and Joze, 2007], while y_i should comply with:

$$\dot{y}_i = D_{yi}^{-1} \{A_i \dot{x}_i - \beta_i |\dot{x}_i| |v_i|^{n_i-1} v_i - \gamma_i \dot{x}_i |v_i|^{n_i}\} \quad (4)$$

where A_i , β_i , and γ_i are the Bouc–Wen [Faycal and Joze, 2007] model parameters that govern the scale, general shape, and smoothness of the hysteresis loop, respectively. In the state space, Equation (2) becomes:

$$Z(t) = \begin{Bmatrix} \{x(t)\} \\ \{\dot{x}(t)\} \end{Bmatrix} \quad (6a)$$

$$g(Z(t)) = \begin{bmatrix} \dot{x}(t) \\ -[M]^{-1}(F_S + C\dot{x}(t)) \end{bmatrix}_{2n \times 2n} \quad (6b)$$

$$[B_u] = \begin{bmatrix} [0] \\ [M]^{-1}[\gamma] \end{bmatrix}_{2n \times r} \quad (6c)$$

$$\{B_r\} = \begin{Bmatrix} [0] \\ [M]^{-1}[\delta] \end{Bmatrix}_{2n \times 1} \quad (6d)$$

$$\{\dot{Z}(t)\} = g(Z(t)) + [B_u]\{u(t)\} + [B_r]\ddot{x}_g(t) \quad (5)$$

where $Z(t)$ is a $2n$ state vector; and other matrices are defined as follows:

The assumed control algorithm is one of the most important factors that significantly affect the control system performance. These algorithms are used to find the optimum control force [Soong 1990]. Among different control algorithms, Linear Quadratic Regulator (LQR) Control and Sliding Mode Control are widely accepted in the literature [Utkin, 1992, Yang et al. 1994, Yang et al. 1995]. It should be mentioned that the Ricatti matrix is obtained by neglecting external excitation $\ddot{x}(t)$ and linearizing the structure at $Z = 0$ [Lee and Chen 2011]. The Sliding Mode Control algorithm is briefly described in the following.

3.2 Sliding mode control

The theory of Variable Structure System (VSS) or Sliding Mode Control (SMC) methods were developed for nonlinear and hysteretic civil engineering structures subjected to intense earthquakes. Here, the emphasis is placed on continuous sliding mode control (CSMC) because of no undesirable chattering effects and continuous characteristics of the control force. The chattering phenomenon is the main drawback in sliding mode controllers. So, CSMC is based on defining appropriate sliding sectors with their respective control rules [Katebi and Zamen 2016]. To find the sliding surface, either the pole assignment or LQR methods can be used. However, the pole assignment method requires pre-specified values of the poles of the system on the sliding surface. Lyapunov stability theory [Utkin 1992] is often applied to obtain control force. Proper design of the sliding surface is basic and usually the most important step of this theory. The sliding surface S is usually regarded as a linear function of state vector Z by means of the following Equation:

$$S = PZ = 0 \quad (7)$$

in which $S = [S_1, S_2, \dots, S_r] = 0$ is an r -dimensional vector, and P is sliding surface coefficient, which is an $(r \times 2n)$ matrix. To determine matrix P , one approach is to convert the state space Equation (5) into the so-called regular form by a transformation matrix D [Yang et al. 1994,1995] as follows:

$$Y = DZ \text{ or } Z = D^{-1}Y \quad ; \quad DB_u = \begin{bmatrix} 0 \\ B_2 \end{bmatrix} \quad (8)$$

where B_2 , an $(r \times r)$ matrix, is non-singular and submatrix of Bu matrix and corresponds to DOF where the controllers are installed. The transformation matrix D , plays the main role herein, which can be obtained using the so-called QR factorization or transformation matrix proposed by Utkin Equation (9) [Utkin 1992]

$$D = \begin{bmatrix} I_{2n-r} & -B_1B_2^{-1} \\ 0 & I_r \end{bmatrix}; \quad D^{-1} = \begin{bmatrix} I_{2n-r} & B_1B_2^{-1} \\ 0 & I_r \end{bmatrix}; \quad B_u = \begin{bmatrix} B_1 \\ B_2 \end{bmatrix} \quad (9)$$

In the design of S , the external excitation and the restoring force in Equation (5) are neglected. However, these two parameters are considered in the calculation of the control force. By applying matrix D to Equations (7) and (8) the equation (5) changes to Equations (10-12):

$$\dot{Y} = \bar{A}Y + \bar{B}_u U \quad (10)$$

$$S = \bar{P} Y = 0 \quad (11)$$

where:

$$\bar{A} = DAD^{-1}; \quad \bar{P} = PD^{-1}; \quad \bar{B}_u = \begin{bmatrix} 0 \\ B_2 \end{bmatrix} \quad (12)$$

By separating those DOFs equipped to controllers from the others, these blocks of the above matrices will be as following Equation (13):

$$Y = \begin{bmatrix} Y_1 \\ Y_2 \end{bmatrix}; \quad \bar{A} = \begin{bmatrix} \bar{A}_{11} & \bar{A}_{12} \\ \bar{A}_{21} & \bar{A}_{22} \end{bmatrix}; \quad P = [\bar{p}_1 \quad \bar{p}_2] \quad (13)$$

where Y_1, Y_2 are $(2n - r)$ and r vectors, respectively; and $\bar{A}_{11}, \bar{A}_{22}, \bar{p}_1$, and \bar{p}_2 are $(2n - r) \times (2n - r)$, $(r \times r)$, $r \times (2n - r)$, and $(r \times r)$ matrices. From Equation (10) to Equation (13) one obtains:

$$\dot{Y}_1 = \bar{A}_{11}Y_1 + \bar{A}_{12}Y_2 \quad (14)$$

$$S = (\bar{P}_1Y_1 + \bar{P}_2Y_2) = 0 \quad (15)$$

Combining Equation (14) and Equation (15) yields the following Equation that is well known as the Equation of motion on the sliding surface:

$$\dot{Y}_1 = (\bar{A}_{11} - \bar{A}_{12}(\bar{P}_2)^{-1}\bar{P}_1)Y_1 \quad (16)$$

In Equation (16), \bar{P}_2 can be chosen as an identity matrix I_r without loss of generality, and the Equation becomes as (Yang et al. 1995):

$$\dot{Y}_1 = (\bar{A}_{11} - \bar{A}_{12}\bar{P}_1)Y_1 \quad (17)$$

The usual procedure for the determination of \bar{P}_1 is the LQR or pole assignment method. Both methods are explained by Yang et al. (1994, 1995). Since the structural properties are assumed to be invariable, the sliding surface remains constant during the control period (Yang et al. 1995). The controller $u(t)$ is designed to force the state trajectory into the sliding surface $S=0$. Therefore, the derivative of the Lyapunov function [Utkin 1992] $V = 0.5 S' S$ must be negative.

$$\dot{V} = S'\dot{S} \leq 0 \quad (18)$$

Constraining the derivative of S by Equation (5) yields to the following continuous controller:

$$u(t) = -(PB_u)^{-1}[g(Z(t)) + [B_r]\ddot{x}_g(t)] - \delta(PB_u)^T S \quad (19)$$

where δ is sliding margin, which is an $(r \times r)$ diagonal matrix with elements $\delta, \delta_2 \dots \delta_r$. The first part of Equation (19) is the equivalent control force obtained from $S'S = 0$. It is observed that $u(t)$ is concerned with restoring force $g(Z(t))$ and ground acceleration $\ddot{x}_g(t)$. When the control force is extremely large (for example, because the designated poles of the sliding surface are quite far from the natural properties of the structural system or because of strong earthquake), the estimated equivalent control force is modulated by a reduction factor α^* which is specified by the designer in the range of $0 \leq \alpha^* \leq 1$. Thus, the control force will be modified as following [Yang et al. 1995]:

$$u(t) = -\alpha^*\{(PB_u)^{-1}[g(Z(t)) + [B_r]\ddot{x}_g(t)]\} - \delta(PB_u)^T S \quad (20)$$

4 Structural Model of the Isolated Bridge

Assuming that the deck of the isolated bridge is rigid, a column with the effective deck mass on top was taken apart as a unitary structural module for seismic analysis, as shown in Figure 4. This column-isolator-deck system can be idealized as a two-DOF lumped mass system. The proposed model indicates that the first DOF is associated with the column. While for the second one, the mass of bearings is negligible compared to deck mass. Accordingly, the mass of the deck has been allocated for this DOF. The column and the isolator are assumed to be perfect elastoplastic and bilinear elastoplastic, respectively. The Bouc-Wen [Faycal and Joze 2007] hysteretic model is used for both column and isolator to measure the stiffness restoring force (Equations (3) and (4)). The column displacement relative to the ground x_c and the isolator displacement relative to the column x_b are the two DOFs, and the deck displacement is regarded as $x_c + x_b$ [Lee and Kawashima 2006]. In this study, a five-span continuous isolated viaduct designed based on Japan Design Specification of Highway Bridges is analyzed to investigate the effectiveness of structural control.

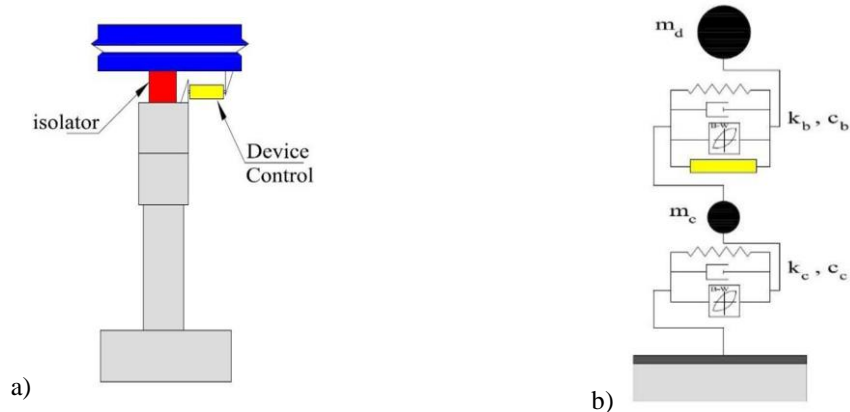


Figure 4 - Analytical idealization of isolated bridge (a) Analytical unit of column and deck, (b) Two DOF system

The schematic shape of the isolated bridge and its superstructure and column and abutments dimension is shown in Figure 5; It should be noted that the dimensions are not scaled in this figure. Five isolators with the size of 112 mm × 600 mm × 600 mm ($H \times B \times D$) support the deck per column or abutment at the ends. The effective mass of the deck and the column are 600 tons and 243.15 tons, respectively. As mentioned earlier, the restoring force of the column and the isolators are perfect elastoplastic and bilinear elastoplastic; the parameters used for the Bouc-Wen model are listed in Table 2. All the following results come from the numerical analysis in MATLAB software. The computations are mainly based on the equations provided in the Control System section.

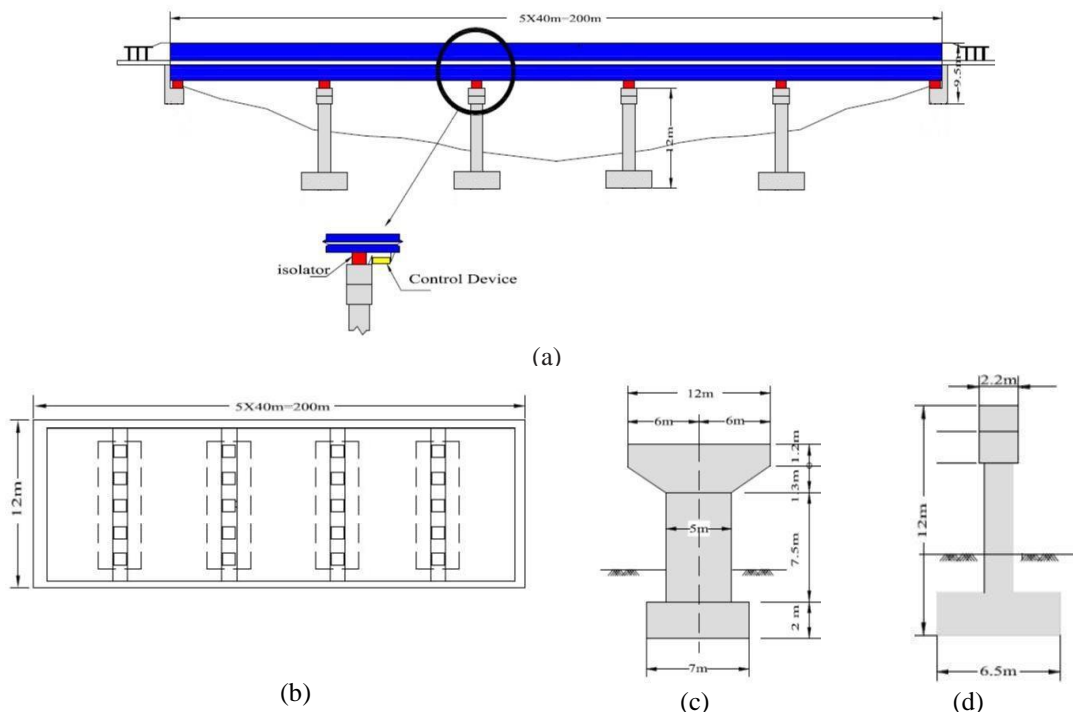


Figure 5 - A five-span isolated viaduct: (a) elevation, (b) plan of superstructure, (c) Lateral view of column, (d) side view of column

Table 2 - *Bouc-Wen model parameters used in isolated bridge*

	Initial Stiffness $k_i \left(\frac{MN}{M}\right)$	Yield Dis. D_{yi} (m)	Bouc-Wen Model Parameters				
			α_i	A_i	β_i	γ_i	n_i
Column	112.7	0.0309	0	1	0.5	0.5	95
Isolator	47.6	0.016	0.191	1	0.5	0.5	95

The first and second natural periods of this bridge is 0.857 s and 0.24 s. The damping ratios of the system are assumed to be 2% for both modes. In this case, the first and second mode shapes would be $\phi_1 = [1, 3.0934]^T$ and $\phi_2 = [1, -0.131]^T$, respectively. In simulations, the isolated bridge is subjected to ET records and a set of ordinary ground motions.

5 Scaling of Ground Motions and ET Functions

The reference set of seven records is referred to as GM set hereinafter, and it is utilized for comparison purposes. These records are used to generate the ETA20e acceleration functions, which are scaled in such a way that the spectrum of each individual record matches the design spectrum of ISS 2800 code (2015) at different excitation levels between $0.2T_i$ and $1.5T_i$ with; where T_i is the fundamental period of vibration of the bridge. Two levels of earthquake hazard are considered, namely those with 10% in 50 years and 2% in 50 years probability of exceedance. These levels of excitations are termed IM1 and IM2, respectively. Since the intensity and magnitude of the earthquake play a pivotal role in nonlinear analysis, this scaling method results in more compatibility between the response spectra of each record along with the associated hazard level [Estekanchi and Basim 2011]. Scale factors obtained using this method are given in Table 3. As mentioned before, various seismic hazard levels can be correlated to equivalent time in ET analysis. These target times should be calculated for comparing ET results with time history analysis. The same procedure has been implemented to identify the equivalent endurance time in ET records corresponding to each hazard level.

 Table 3 - *The scaling factors used for the selected ground motions*

Record	Scale factors	
	10% in 50 year (IM1)	2% in 50 year (IM2)
LADSP000	2.349	3.524
LPSTG000	1.148	1.723
LPGIL067	1.531	2.182
LPGLOB000	1.415	2.123
LPAND270	1.641	2.462
MHG06090	1.052	1.577
NRORR360	0.645	0.968

With few trial and error, these equivalent times can be readily calculated due to the linear intensification scheme of ET method. These values are given in Table 4. The mean acceleration response spectrum of the scaled GM records and ETAFs is shown in Figure 6 with the target response spectrum at different excitation levels on the same plot.

Table 4 - Equivalent time corresponding to each hazard level

Probability of exceedance (%)	Equivalent target time in ET method (s)		
	ETA20e01	ETA20e02	ETA20e03
10% in 50 year (IM1)	6.15	6.74	6.05
2% in 50 year (IM2)	9.78	9.18	9.67

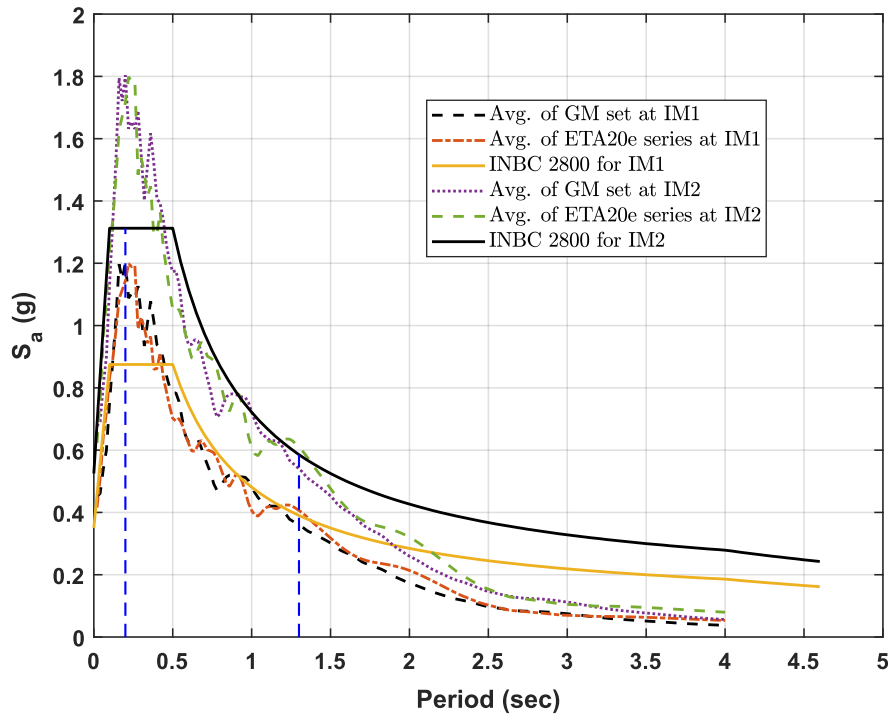


Figure 6 - Scaled ETAFs and GM set and INBC 2800 at different hazard levels

6 Numerical Simulations

The different performances and the corresponding mitigation of the deck displacements given by active, semi-active, and passive control systems are obtained from the numerical simulations summarized herein. The following index for deck displacement is introduced to evaluate the performance of these systems:

$$j_d = \frac{\max|x_{du} - x_{dc}|}{\max|x_{du}|} \quad (21)$$

where x_{dc} and x_{du} are the deck displacement with and without control, respectively.

6.1 Active system

The active system is used for both CSMC and LQR control, and their performances are compared with each other. For the sliding surface design, both the LQR and pole assignment method is used. For calculation of the sliding surface, the weighting matrix Q is assumed as a diagonal matrix, i.e., $Q = [1,1000,1,1]$. It should be noted that the weighting matrix Q is chosen in such a way to reduce the isolator displacement more than the column. By solving Equation (21) using LQR method, the sliding surface would be as $S = -4.25x_c + 22.36x_b + 0.48\dot{x}_c + 1.21\dot{x}_b$ in which the pole corresponding to this Q matrix on the sliding surface results in $[-27.09, -1.3 + 11.198i, -1.3 - 11.198i]^T$. The real parts of poles on the sliding surface are negative, which ensures the system stability after control. Usually, the maximum control force is expressed as a percentage of the total structure. As mentioned earlier, in this study, the control force is assumed to be 30% of the deck weight, i.e., something around 1800 kN. Another approach for the design of the sliding surface is using the pole placement method. So, three poles are selected as $[-30, -5 + 10i, -5 - 10i]^T$ on the sliding surface. These poles are selected among trial and error done by Lee and Chen (2011). In this case, the sliding surface equation would be $S = 197.46x_c + 199.71x_b + 14.89\dot{x}_c + 11.82\dot{x}_b$. In the pole assignment method, the coefficients of matrix P are much greater than those gained by the LQR method. So the α^* is taken fairly smaller in pole assignment method. To show the robustness of CSMC, the traditional LQR control (LQRC) is used. In the LQRC algorithm, the weighting matrix Q is identical to that used for CSMC, whereas the weighting matrix R is adjusted so that the maximum control force becomes 30% of the deck weight.

6.2 Semi-active system

The concept of semi-active control is investigated as another control system herein. To apply the control force to the bridge, a variable viscous damper is selected as the semi-active device. These dampers contain a hydraulic cylinder and a piston, which can vary the damping coefficient. In fact, the damping characteristic of the damper can be controlled by varying the amount of the viscous material, which passes through the by-pass [Kawashima and Unjoh 1994]. The control force exerted from a variable viscous damper is given by Maxwell model [Symans and Constantinou 1999] as follows:

$$F_v(t) = c_v(t)\dot{x}_b(t) \quad (22)$$

where $c_v(t)$ is the time-variant damping coefficient, and $\dot{x}_b(t)$ is the relative velocity of the isolator. It is noted that $c_v(t)$ is bounded by a minimum and maximum value as:

$$c_{vmin} \leq c_v(t) \leq c_{vmax} \quad (23)$$

Equating the control force in Equation (22) and desired optimal control leads to:

$$c_v^*(t) = \frac{U(t)}{\dot{x}_b(t)} \quad (24)$$

Therefore, the damping coefficient in Equation (22) modifies in each cycle as the following constrain:

$$c_v(t) = \begin{cases} c_{vmin} & c_v^* \leq c_{vmin} \\ c_v^* & c_{vmin} \leq c_v^* \leq c_{vmax} \\ c_{vmax} & c_v^* \geq c_{vmax} \end{cases} \quad (25)$$

The minimum and maximum amount of this coefficient are bounded as $c_{vmax} = 4MN$ and $c_{vmin} = 1MN$, respectively [Lee and Chen 2011]. As a result, the control forces for previous study cases (LQR and CSMC) are updated based on the new damping coefficient in each control cycle.

6.3 Passive system

In addition to the aforementioned control systems, allocating the absolute value of c_{vmin} and c_{vmax} as damping coefficient yields passive control force. In other words, the control force would be a function of isolator's relative velocity. The allocated amounts for maximum and minimum of damping coefficient are the same as the semi-active case, i.e., as $c_{vmax} = 4MN$ and $c_{vmin} = 1MN$ [Lee and Chen 2011].

7 Results and Discussion

The main performance parameters that are monitored from the analyses are the deck displacements. For analysis of bridge using ET method, e-series of ETAFs have been used. Furthermore, the average maximum results of seven scaled ground motions (GM) have been computed and considered as reference. For each set, the mean value and standard deviation of the specified response can be calculated as follows:

$$\overline{EDP} = \frac{1}{n} \sum_{i=1}^n EDP \quad (26)$$

$$\sigma = \sqrt{\frac{\sum_{i=1}^n (EDP - \overline{EDP})^2}{n - 1}} \quad (27)$$

where EDP is the desire response parameter, n is the number of ground motions, \overline{EDP} is the mean value of EDPs, and σ is the standard deviation. In order to determine the maximum of each EDP at any time in ET method, the maximum absolute value of the response up to the intended time is calculated. This procedure is illustrated for active SMC system in Figure 7.

In Figure 8, the ET diagram for three ET records (ETA20e01-3) and also discrete values of the average of the time-history analysis with one standard deviation for each intensity level is shown for active SMC system. This figure indicates that ET analysis can estimate deck displacement at different intensity levels with acceptable accuracy.

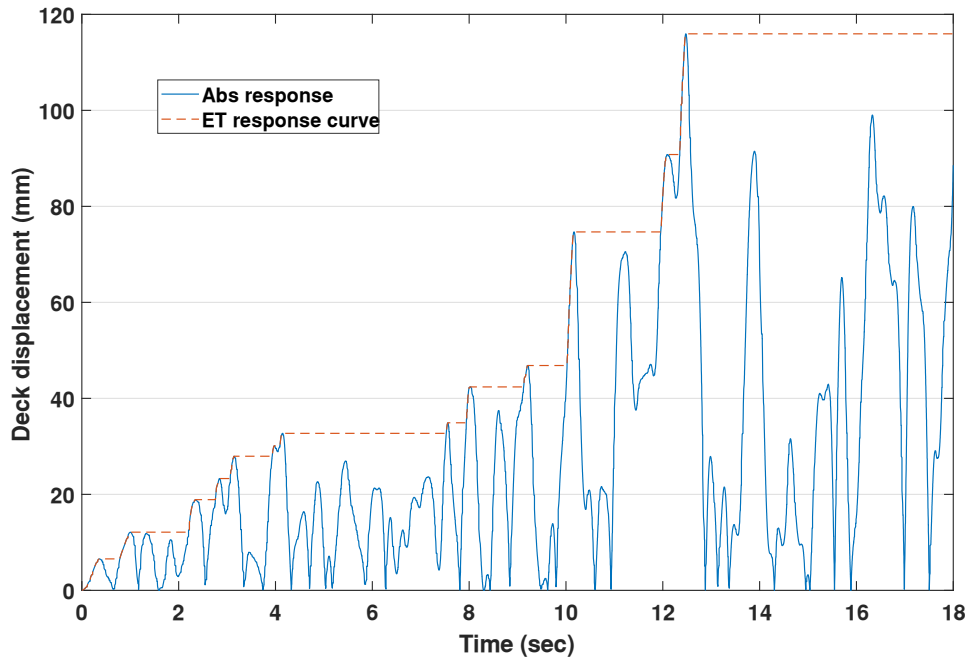


Figure 7 - Method of obtaining ET diagram

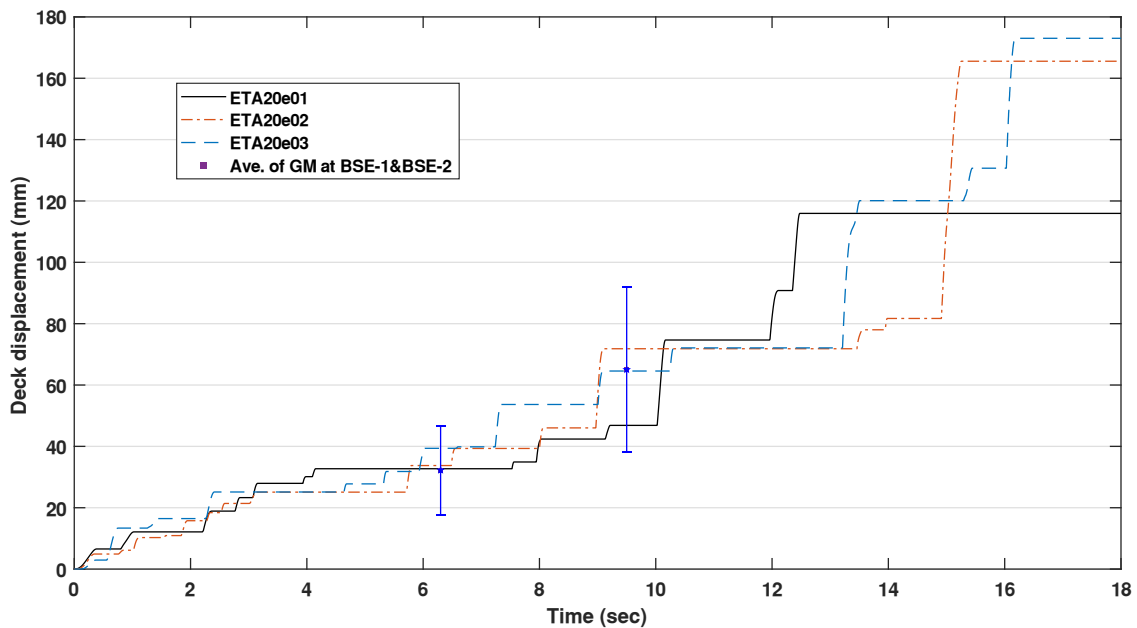


Figure 8 - ET diagram for deck displacement

Figure 9 summarizes the comparison of different control systems in mitigating deck displacement at different intensity levels for ET method as well as time history analysis. As expected, the active SMC system has the best performance compared to other control systems, which denotes the robustness of continuous sliding mode control. These results are consistent with the results reported in the literature [Utkin 1992, Yang et al. 1994, Yang et al. 1995, Lee and Kawashima 2006, Lee and Chen 2011].

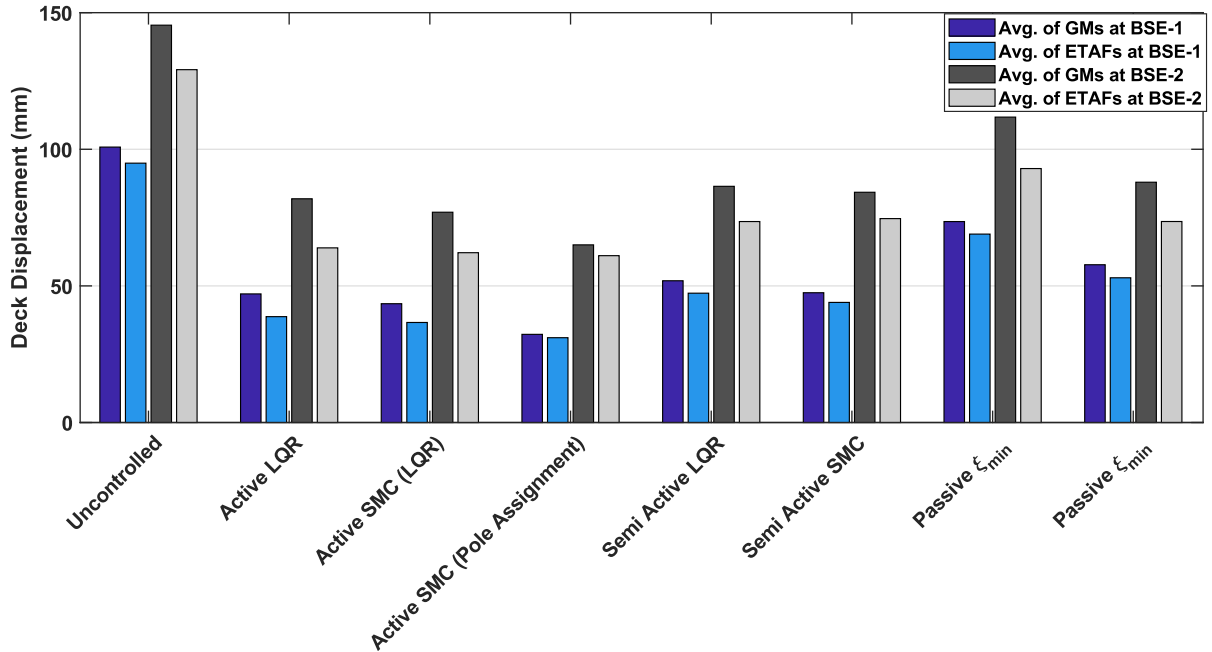


Figure 9 - Average of maximum deck displacements from time history analysis and ET method for different control systems

On the basis of the obtained results in Figure 9, the following observations can be made:

- Similar to time history analysis, ET method illustrates that an active SMC system has the best performance in reducing deck displacement.
- For all control systems at different intensity levels, ET analysis gives smaller deck displacements than time history analysis. This is mainly due to the fact that at periods of vibration of the bridge, the mean response spectra of ETAfs fall below the response spectrum of GM set.

The results for different control systems under scaled selected records and series ETA20e013 of ET acceleration functions are summarized in Table 5 and Table 6 along with the error between these two groups, which are computed as follows:

$$Err \% = \frac{|EDP_{Gm} - EDP_{ET}|}{EDP_{Gm}} \times 100 \quad (28)$$

in which EDP_{Gm} is the intended parameter obtained from GM set, and EDP_{ET} is the same for ET method. According to J index, active SMC pole assignment has the best performance in reducing the deck displacement by 67% and 53% at both intensity levels, respectively. The results from ET method also follow the same pattern at both excitation levels. The difference values (error) are generally below 10% and 20% at IM1 and IM2 level, respectively, which denotes the capability of ET method in estimating the mean response of the structure with reasonable accuracy. The hysteretic loops of the isolator and the column are shown in Figure 10 for the cases uncontrolled and active SMC; which demonstrates that the demand isolator and column ductility becomes smaller under the active SMC for both time-history and ET method.

Table 5 - Summary of the analysis results at IM1

Records	Uncontrolled	Active (LQR)	Active SMC (LQR)	Active SMC (Pole Assignment)	Semi Active (LQR)	Semi Active (SMC)	Passive with ξ_{min}	Passive with ξ_{max}
Scaled ground motion								
LPAND270	7.132	6.859	6.375	7.899	6.96	7.371	8.951	6.984
LADSP000	8.883	4.263	3.783	3.009	4.656	4.406	5.123	4.297
NRORR360	10.947	5.259	4.743	1.205	6.177	4.781	8.928	6.783
LPGIL067	9.037	4.103	3.72	3.226	4.047	4.142	6.415	5.876
MHG06090	11.319	6.078	4.534	3.214	6.366	4.879	8.802	6.259
LPSTG000	15.754	6.423	6.89	6.092	7.114	7.034	11.085	8.266
LPGLOB000	7.491	2.819	2.819	2.661	3.137	3.228	5.073	4.037
Avg. GM	10.08	4.71	4.35	3.23	5.19	4.75	7.35	5.77
Dis. Index	-	53%	57%	68%	49%	53%	27%	43%
STDEV	2.96	1.28	1.28	1.45	1.41	1.16	2.28	1.5
ET results								
ETg_01	8.868	4.171	3.297	3.125	3.699	3.554	5.681	4.2
ETg_02	8.255	3.584	3.774	3.236	4.811	4.706	6.595	5.44
ETg_03	11.353	3.869	3.913	2.951	5.689	4.927	8.411	6.251
Avg. ET	9.49	3.87	3.66	3.1	4.73	4.4	6.9	5.3
Dis. Index (%)	-	59%	61%	67%	50%	54%	27%	44%
STDEV	1.64	0.29	0.32	0.14	1	0.74	1.39	1.03
Error bar (%)	5.85%	17.83%	15.86%	4.02%	8.86%	7.37%	6.12%	8.15%

Table 6 - Summary of the analysis results at IM2

Records	Uncontrolled	Active (LQR)	Active SMC (LQR)	Active SMC (Pole Assignment)	Semi Active (LQR)	Semi Active (SMC)	Passive with ξ_{min}	Passive with ξ_{max}
Scaled ground motion								
LPAND270	12.124	6.859	6.375	7.899	6.96	7.371	8.951	6.984
LADSP000	9.465	6.469	7.123	8.431	7.052	7.806	8.651	7.415
NRORR360	14.194	9.271	8.041	5.609	9.812	8.284	12.505	9.596
LPGIL067	16.448	6.828	7.939	10.407	7.268	8.613	11.223	9.624
MHG06090	18.401	10.443	7.9	6.515	9.992	8.582	13.296	8.771
LPSTG000	21.878	12.554	11.505	2.52	14.415	13.556	17.145	13.199
LPGLOB000	9.283	4.894	4.992	4.132	5.011	4.775	6.471	5.972
Avg. GM	14.54	8.19	7.7	6.5	8.64	8.43	11.18	8.79
Dis. Index	-	44%	47%	55%	41%	42%	23%	40%
STDEV	4.69	2.67	2	2.68	3.08	2.62	3.54	2.38
ET results								
ETg_01	13.157	6.233	5.8174	4.683	7.361	5.218	10.354	7.552
ETg_02	14.156	6.421	6.398	7.18	7.24	7.915	9.119	8.267
ETg_03	11.427	6.521	6.429	6.456	7.471	7.011	8.411	6.251
Avg. ET	12.91	6.39	6.21	6.11	7.36	6.71	9.29	7.36
Dis. Index (%)	-	51%	52%	53%	43%	48%	28%	43%
STDEV	1.38	0.15	0.34	1.28	0.12	1.37	0.98	1.02
Error bar (%)	11.21%	21.98%	19.35%	6.00%	14.81%	20.40%	16.91%	16.27%

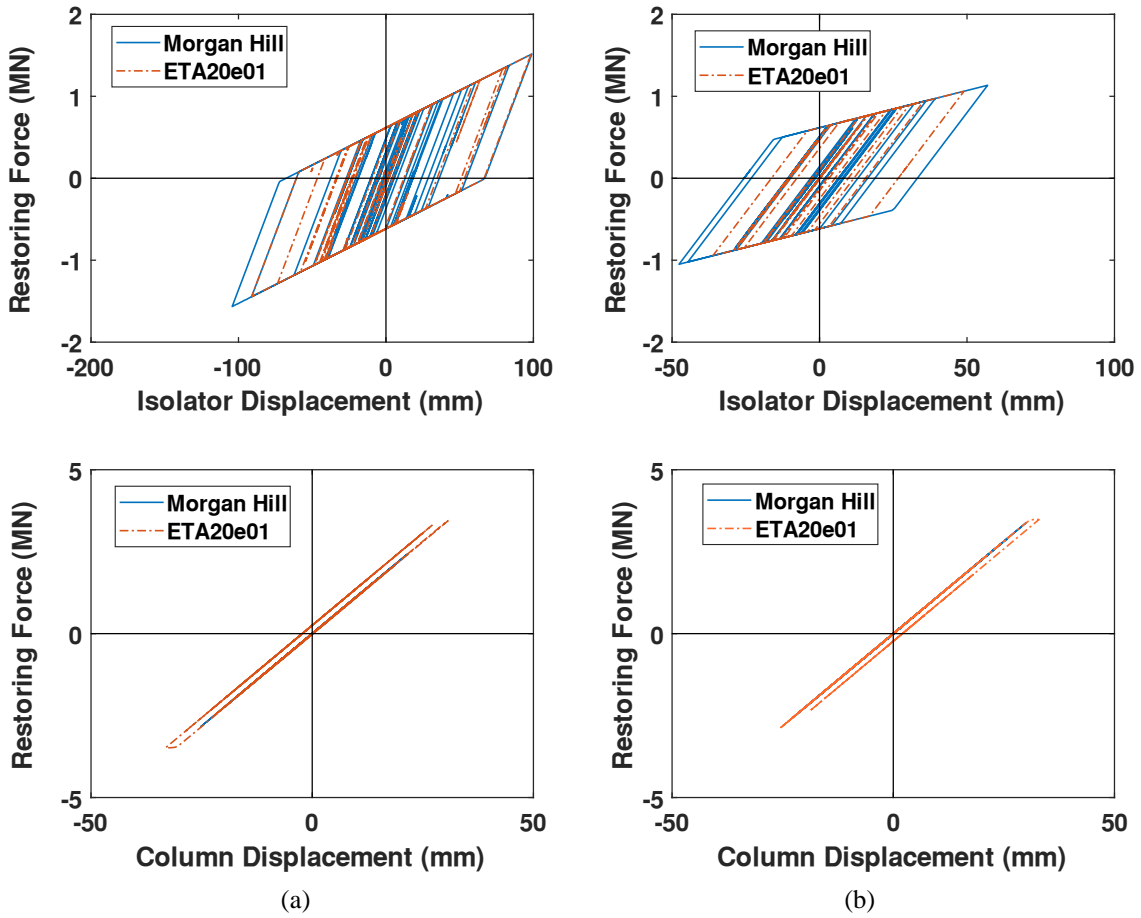


Figure 10 - *Hysteretic loops of the isolator and the column: (a) Uncontrolled, (b) Active SMC*

Figure 11 compares the mean value and the mean plus and minus standard deviation of maximum deck displacement obtained by ET method and time history analysis. As it can be observed, the data points for time history analysis have a larger scatter.

This result can be partially attributed to the fact that ground motions come from different events with different faulting mechanisms and geological conditions. On the contrary, ETAFs are produced artificially in such a way that their response spectrum is matched directly to a target response spectrum in the optimization process.

Figure 12a and b show a comparison between the control force and the deck displacement response of the isolated bridge among uncontrolled, active, and semi-active controlled systems under Morgan Hill accelerograms and ETA20e01 acceleration function. The associated semi-active damping coefficient of the variable viscous damper is also depicted in this figure for both time history analysis and ET method. The results from these simulations demonstrate the applied control force can be approximately generated by variable viscous damper in most time. It is noteworthy to point out that the limitation of the damping coefficient causes the discrepancy between the applied damping force and the desired control force in some time.

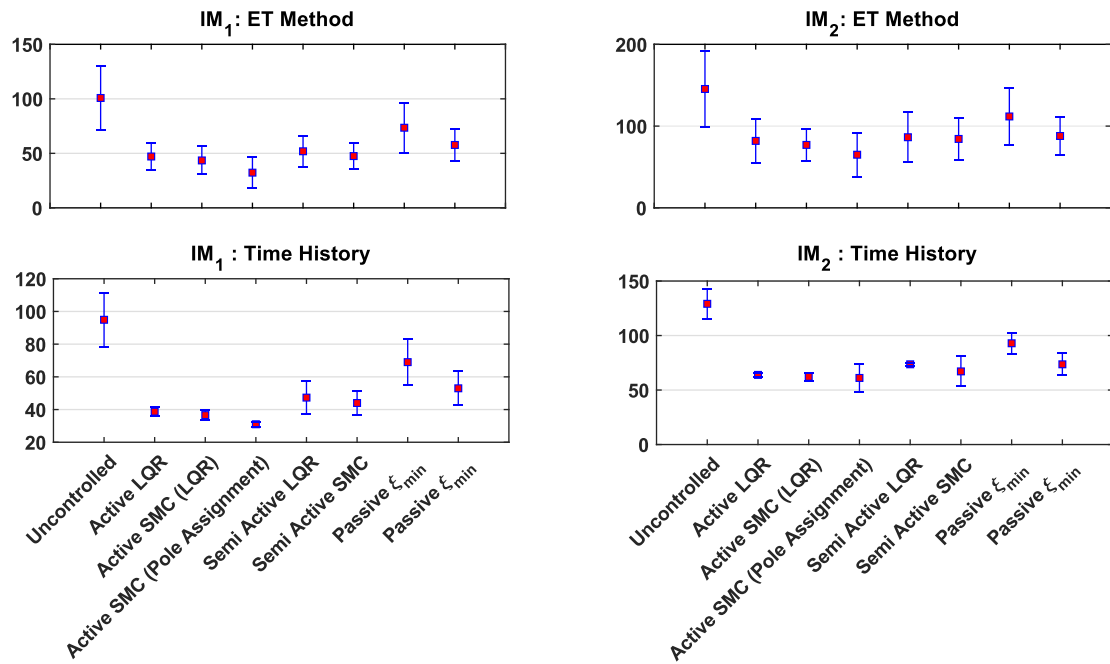


Figure 11 - Maximum deck displacement considering one +/- standard deviation at IM1 and IM2 hazard level for ET method and time history analysis

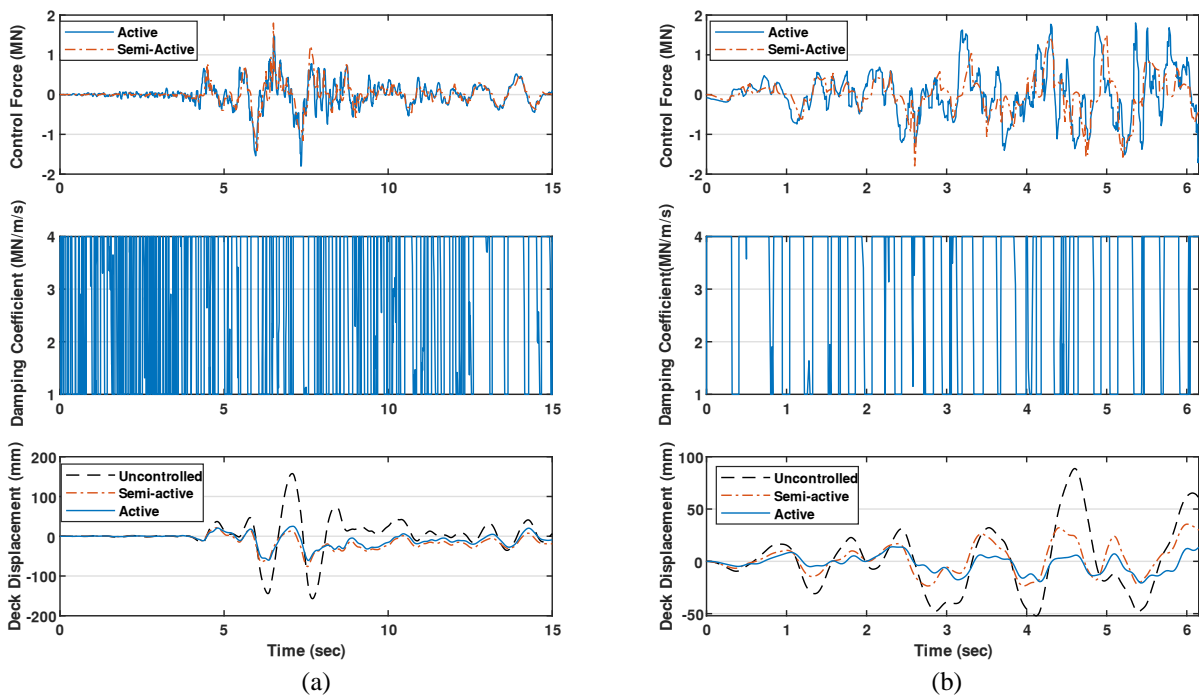


Figure 12 - Comparison of the control force, damping coefficient of the variable damper, and deck displacement between active and semi-active control based on sliding mode control: (a) Morhan-Hill, (b) ETA 20e01

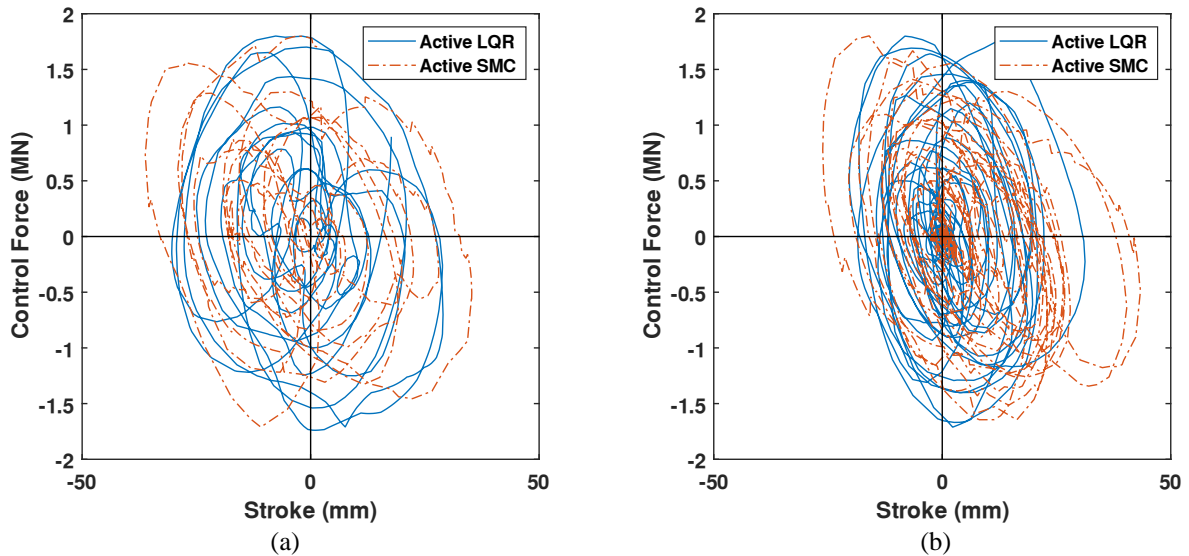


Figure 13 - *Hysteretic loops of the actuator for active LQR and active SMC: (a) Morgan Hill (b) ETA20e01 record*

As an example, the hysteresis loops of control force obtained from ETA20e01 acceleration function until 9.78 seconds (which is equivalent to 2% in 50 years earthquake) and Morgan accelerograms for active LQR and CSMC systems are depicted in Figure 13. One notable feature of this figure is that the number of hysteretic loops of ETA20e01 acceleration function is fewer than the Morgan accelerogram. Although ET curves show fewer cycles compared to time- history analysis, maximum values for both methods are close to each other.

8 Conclusions

In current engineering design practice, the conventional nonlinear time history analysis is the most accurate and reliable approach to seismic analysis. However, the computational cost of performing a sufficient number of time history analyses to reach a high degree of precision can become a heavy burden. On the contrary, the ET method is an innovative, dynamic analysis that represents an easier and more practical method compared to nonlinear time history analysis.

In this paper, the effectiveness of ET method in different control systems is studied for a nonlinear isolated bridge, and the results of ET method and traditional time history are compared with each other at different intensity levels.

Simulation results indicate that ET method is capable of predicting the seismic response of isolated bridge under different control systems with acceptable accuracy. This method avoids the major pitfall in time history analysis, which requires selecting or generating time history ground motions compatible with target response spectrum, while it has no limitation in modeling different structures with different complexity. Furthermore, ET method considerably reduces the computational demands, particularly in evaluating structures for several levels of seismic hazard by providing useful information at different excitation levels in a single time history analysis. For instance, 14-time history analyses have been performed for evaluating the studied bridge at two excitation levels, whereas, in ET method,

approximately the same results have been obtained by only carrying out three analyses. However, since ET uses a pre-design intensifying dynamic excitation, the application of the method is limited to sites that these functions are available. These functions are generated by numerical optimization methods and are publicly available for use (<https://sites.google.com/site/etmethod/>).

It is also noteworthy to indicate that the maximum standard deviations in ET method are 1.64 and 1.38, whereas the corresponding value for time history analysis are 2.96 and 4.69 at IM1 and IM2. Due to this fact, it seems even reasonable to achieve the preliminary design based on one ET analysis.

References

- Basim, M.Ch., Estekanchi, H., & Mahsuli, M. (2018). Application of first-order reliability method in seismic loss assessment of structures with Endurance Time analysis. *Earthquakes and Structures*, 14(5):437-447.
- Bedon, C., & Morassi, A. (2014). Dynamic testing and parameter identification of a base-isolated bridge. *Engineering Structures*, 60:85-99.
- Bernuzzi, C., Crespi, P., Montuori, R., Nastri, E., Simoncelli, M., Stochino, F., Zucca, M. (2021) Resonance of steel wind turbines: Problems and solutions. *Structures*, 32: 65-75.
- Colajanni, P., Cacciola, P., Potenzzone, B., Spinella, N., & Testa, G. (2017). Non linear and linearized combination coefficients for modal pushover analysis. *Ingegneria Sismica*, 34, 93-112.
- Corbi, I., Corbi, O., & Li, H. (2019). A coupled control strategy for the mitigation of structural vibrations. *Ingegneria Sismica*, 36(3), 107-115.
- Estekanchi, H. & Alembagheri, M. (2012). Seismic analysis of steel liquid storage tanks by Endurance Time method. *Thin-Walled Structures*, 50(1):14-23.
- Estekanchi, H. & Basim, M. Ch. (2011). Optimal damper placement in steel frames by the Endurance Time method. *The Structural Design of Tall and Special Buildings*, 20(5):612–630.
- Estekanchi, H., Valamanesh, V., & Vafai, A. (2007). Application of endurance time method in linear seismic analysis. *Engineering Structures*, 29(10):2551–2562.
- Fayçal, I. & José, R. (2007). *Systems with Hysteresis Analysis, Identification and Control Using the Bouc-Wen Model*. Wiley-Inter science, USA.
- FEMA-440. (2005) *Improvement of Nonlinear Static Seismic Analysis Procedures*, Federal Emergency Management Agency, Washington (DC).
- Franklin, Y.C., Hongping, J. & Kangyu, L. (2008). *Smart Structures Innovative Systems for Seismic Response Control*, CRC Press, USA.
- Ferraioli, M., Lavino, A., & Mandara, A. (2018). Effectiveness of multi-mode pushover analysis procedure for the estimation of seismic demands of steel moment frames. *Ingegneria Sismica*, 35(2), 78-90.
- Fraternali, F., Amendola, A., Benzoni, G. (2018) Innovative seismic isolation devices based on lattice materials: A review [Dispositivi di isolamento sismico innovativi basati su materiali reticolari: Studio di letteratura] *Ingegneria Sismica*, 35 (4): 93-113.
- Gabbianelli, G., Cavalieri, F., Nascimbene, R. (2020) Seismic vulnerability assessment of steel storage pallet racks. *Ingegneria Sismica*, 37 (2): 18-40.
- Katebi, J., & Zamen, S. (2016). Robust time varying sliding sector for uncertain structures control, *Journal of Vibration and Control*, 24(1):171- 190.

- Kawashima, K. & Unjoh, S. (1994). Seismic response control of bridges by variable dampers, *Journal of Structural Engineering*, ASCE 120(9):2583–2601.
- Lee, T.Y., & Chen, P.C. (2011). Experimental and analytical study of sliding mode control for isolated bridges with MR dampers. *Journal of Earthquake Engineering*, 15(4):564-581.
- Lee, T.Y., & Chen, P.C. (2011). Sliding mode control for nonlinear isolated bridges. *Journal of Earthquake Engineering*, 15(4):582-600.
- Lee, T.Y., & Kawashima, K. (2006). Effectiveness of seismic displacement response control for nonlinear isolated bridge. *Structural Engineering / Earthquake Engineering*, 23(1):1-15.
- Liao, W.I., Loh, C.H., & Lee, B.H. (2004). Comparison of dynamic response of isolated and non-isolated continuous girder bridges subjected to near-fault ground motions. *Engineering Structures*, 26(14):2173–2183.
- Losanno, D., Hadad, H.A., & Serino, G. (2017). Seismic behavior of isolated bridges with additional damping under far-field and near fault ground motion. *Earthquakes and Structures*, 13(2):119-130.
- Mao, Y., Tremblay, R., Léger, P., & Li, J. (2017). New simplified method for designing seismically isolated highway bridges with massive piers. *Journal of Bridge Engineering*, 22(8): 04017041.
- Mirzaee, A., & Estekanchi, H. (2015). Performance-Based seismic retrofitting of steel frames by the endurance time method. *Earthquake Spectra*, 31(1):383-402.
- Montuori, R., Nastri, E., & Tagliafierro, B. (2021). Residual displacements for non-degrading bilinear oscillators under seismic actions. *Mechanics Research Communications*, 111, 103651.
- Riahi, H.T. & Estekanchi, H. (2007). Comparison of different methods for selection and scaling of ground motion time histories. 5th International Conference on Seismology and Earthquake Engineering, Tehran, Iran.
- Shen, J., Tsai, M.H., Chang, K.C., and Lee, G.C. (2004). performance of a seismically isolated bridge under near-fault earthquake ground motions. *Journal of Structural Engineering*, 130(6):861-868.
- Soong, T.T. (1990). *Active Structural Control: Theory and Practice*, Longman structural engineering and structural mechanics series, England.
- Standard No. 2800 (2015), Iranian Code of Practice for Seismic Resistant Design of Buildings, 4th edition, Building and Housing Research Center, Tehran, Iran.
- Symans, M.D. & Constantinou, M.C. (1999). Semi-active control systems for seismic protection of structures: a state-of- the review. *Engineering Structures*, 21(6):469-487.
- Terenzi, G., Sorace, S., Spinelli, P., & Rossi, E. (2019). Seismic protection of a historical R/C elevated water tank by different base isolation systems. *INGEGNERIA SISMICA*, 36(2), 137-158.
- Utkin, V.I. (1992). *Sliding Mode in Control Optimization*, Springer Verlag, New York, NY, USA.
- Yang, J.N., Wu, J.C, Agrawal, A.K., & Li, Z., (1994). Sliding mode control for seismic-excited linear and nonlinear civil engineering structures. (NCEER-94-0017), National Control for Earthquake Engineering: State University of New York, Buffalo.
- Yang, J.N., Wu, J.C. & Agrawal, A.K. (1995). Sliding mode control for nonlinear and hysteretic structures. *Journal of Engineering Mechanics*, 121(12):1330-1339.
- Yu, Y, Royel, S., Li, J., Li, Y. & Ha, Q. (2016). Magnetorheological elastomer base isolator for earthquake response mitigation on building structures: modeling and second order sliding mode control. *Earthquakes and Structures*, 11(6):243-966.
- Zanini, M.A., Hofer, L., Faleschini, F., Pellegrino, C. (2017) The influence of record selection in assessing uncertainty of failure rates. *Ingegneria Sismica*, 34 (4): 30-40.



Applicazione del metodo Endurance Time per la valutazione sismica di un viadotto isolato

Hamidreza Nemati¹, Arash Poursadrollah², Javad Katebi¹, Mario D’Aniello², Raffaele Landolfo², Arash Bahar

¹Department of Civil Engineering, University of Tabriz, Tabriz, Iran

²Department of Structures for Engineering and Architecture, University of Federico II, Naples, Italy

³Department of Civil Engineering, University of Guilan, Guilan Province, Rasht, Iran

SOMMARIO: *Il metodo Endurance Time (ET) consiste di un'analisi dinamica in cui le strutture sono soggette ad una predefinita e crescente accelerazione. La natura intrinsecamente dinamica di ET lo rende applicabile a vari tipi di strutture con diverse altezze e gradi di libertà. Lo scopo di questo studio è di indagare la fattibilità del metodo ET per analizzare un ponte isolato ed equipaggiato con diversi sistemi controllati. La forza di controllo ottimale viene calcolata utilizzando sia l'algoritmo del regolatore quadratico lineare (LQR) che il controllo della modalità di scorrimento continuo (CSMC). A tal fine, come caso di studio viene selezionato un viadotto isolato di cinque campate. Il sistema colonna-isolatore-ponte è idealizzato come un modello a massa concentrata con due gradi di libertà. Vengono utilizzate tre distinte strategie di controllo, ovvero i sistemi di controllo attivo, semi-attivo e passivo. Gli spostamenti del ponte ottenuti dal metodo ET vengono confrontati con i risultati dell'analisi dinamica al passo per diversi livelli di eccitazione. I risultati dell'ET mostrano una buona accuratezza nella previsione del comportamento sismico di ponti isolati sotto diversi sistemi controllati. Inoltre, questo metodo riduce sostanzialmente le richieste computazionali contrariamente all'analisi dinamica al passo.*

PAROLE CHIAVE: *metodo Endurance Time, ponte isolato, controllo attivo e semi-attivo, analisi dinamica al passo*